

Unraveling the degradation mechanism of FIrpic based blue OLEDs: I. A theoretical investigation

Marco Cazzaniga,^{*,†,¶} Fausto Cargnoni,^{*,†,‡} Marta Penconi,[†] Alberto Bossi,^{†,‡}
and Davide Ceresoli^{*,†,‡}

[†]*Consiglio Nazionale delle Ricerche - Istituto di Scienze e Tecnologie Molecolari, via Golgi
19, 20133 Milano, Italy*

[‡]*Consorzio INSTM, UdR di Milano, Italy*

[¶]*Present address: Department of Chemistry, University of Milan, via Golgi 19, 20133
Milano, Italy*

E-mail: marco.cazzaniga@unimi.it; fausto.cargnoni@istm.cnr.it; davide.ceresoli@cnr.it

Abstract

We report a detailed ab-initio study of the of the microscopic degradation mechanism of FIrpic, a popular blue emitter in OLED devices. We simulate the *operando* conditions of FIrpic by adding an electron-hole pair (exciton) to the system. We perform both static calculations with the TDDFT framework and we also simulate the evolution of the system at finite temperature via Car-Parrinello molecular dynamics. We found triplet excitons are very effective in reducing the Ir-N bond breaking barrier of the picolinate moiety. After the first bond breaking, the two oxygen of picolinate swap their position and FIrpic can either remain stable in an “open” configuration, or loose a picolinate fragment, which at a later stage can evolve a CO₂ molecule. Our method can be applied to other light emitting Ir-complexes in order to quickly estimate their stability in OLED devices. In Paper II we complement our theoretical study with

a parallel experimental investigation of the key degradation steps of FIrpic in an aged device.

Introduction

Organic light-emitting diodes (OLEDs) offer the potential of using both the singlet and triplet excitons in realizing 100% internal quantum efficiencies of electro-luminescence (see Ref.¹ for a recent review). During the operation lifetime of a OLED device, the injected charge carriers (electrons and holes) may become trapped at morphological and chemical defects, and recombine non-radiatively. These phenomena, not only limit the quantum efficiency of the device, but are also responsible for the degradation of the device (leading to aging and failure), through the formation of highly reactive radical species.² The danger of chemical degradation is particularly enhanced in blue-emitting phosphorescent devices, because of the large energy of the photon and of the long lifetime of the excited triplet state.³ Several mechanism are responsible of the degradation of the emission properties of PhOLEDs, either by quenching emission, or by chemical degradation. These include triplet-triplet annihilation (TTA), triplet-polaron annihilation (exciton-charge interaction).^{4,5} These mechanism might not be thermodynamically favorable, but when they take place, they can be as detrimental as non-radiative exciton recombination.

In a real device, under operating conditions, chemical degradation occurs both in the charge-transporting layers (*host*) and in the emissive layers, where *guest* emitting dyes are dispersed. For instance CBP (4,4'-Bis(N-carbazolyl)-1,1'-biphenyl), an efficient hole-transporting material, can trap an extra charge (*polaron*) that can break one of the C–N bonds. The resulting radical fragment is highly reactive and will attach to a neighboring CBP molecule, modifying dramatically its photophysical and transport properties.⁶ The degradation of FIrpic (Bis[2-(4,6-difluorophenyl)pyridinato-C²,N](picolinato)Ir(III)) has been studied experimentally by Moraes and coworkers,⁷ who performed mass spectroscopy experiments

on pristine and aged devices. From the observed fragments, the authors were able to propose two degradation pathways: (i) detachment of the picolate; (ii) loss of a CO₂ molecule and possible sequential loss of the pyridine. They also observed the formation of several Ir complex incorporating ligands from the host molecules. Moreover the presence of all FIrpic isomers was observed in aged devices,⁸ despite the fact that the synthetic route of FIrpic yields only one isomer.⁹

Density Functional Theory (DFT) and its time-dependent DFT (TDDFT) calculations provide a wealth of useful insights into the photodeactivation, inter-system crossing and non-radiative decay processes.^{10-13,13-21} Calculations on Ir(ppy)₃ and Ir(ppz)₃ showed that these complexes display a stable “open” state, in which one of the the ligand break one bond with the central Ir, followed by a rotation of the ligand along the remaining Ir-bond. This open state is particularly favored in the triplet state.²² The isomerization barriers of a small model Ir complex where calculated in Ref.²³ However, the isomerization of larger, emissive Ir-complexes, will require to overcome quite large energy barriers, because of the steric hindrance of the ligands.²⁴ Therefore, a complete understanding of the degradation pathways, based on atomistic modeling, is still missing to date.

In this manuscript we concentrate on the guest emitter FIrpic, whose most stable isomer is shown in Fig. 1. To simulate a OLED *operando* conditions, it is necessary to perform DFT calculations in the charged and excited state. In principle, excited states (singlet or triplet) can be modeled accurately only by many-body perturbation theory such as the GW-BSE technique,^{25,26} but this method is too computationally expensive even on modern supercomputers. Moreover, non-adiabatic evolution of charges and excitons is usually simulated by TDDFT Eherenfest dynamics²⁷ or Tully Surface Hopping.^{28,29} The time step needed for TDDFT propagation is of the order of attoseconds (10⁻¹⁸ s), and the simulation time is restricted to few picoseconds (10⁻¹² s), which is sufficient to simulate fast radiative and non-radiative processes.

To simulate the degradation mechanisms, a much longer timescale (~10 picoseconds)

is needed, corresponding to the time occurring for molecular geometry rearrangements and bond-breaking. Therefore, we perform Car-Parrinello molecular dynamics³⁰ with constrained orbital occupations (c-CPMD). This computational framework was used successfully to simulate electron-polarons,^{31,32} exciton trapping and chemical degradation in crystalline polyethylene.^{33,34} In those works on polyethylene, it was shown that c-CPMD method is accurate enough to provide at least a qualitative picture of the degradation pathways. However, a precise estimate of the probability and the timescale of the degradation process, cannot be obtained with the c-CPMD method. We also performed a series of static computations to simulate the initial step (i.e. bond breaking) of FIrpic. Interestingly, in performing these calculations we discovered a possible mechanism of isomerization of FIrpic requiring relatively low energy barriers.

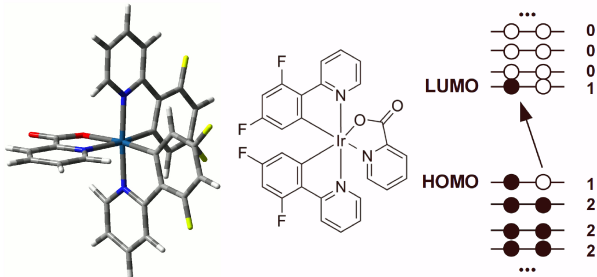


Figure 1: (Left panel) The most stable isomer of the closed FIrpic molecule in its electronic ground state. Hydrogen atoms are painted in white, carbon in grey, nitrogen in blue, oxygen in red, fluorine in yellow, iridium in light blue. (Center panel) FIrpic chemical structure. (Right panel) Schematic representation of the orbital occupations of FIrpic during Car-Parrinello molecular dynamics runs in the excited state.

Computational details

Static computations

We performed static computations (i.e. at zero temperature) of FIrpic in three different electronic states: the singlet ground state (GS); the first excited triplet (T_1), described

both with an unrestricted DFT scheme and the TDDFT method within the Tamm-Dancoff (TDA) approximation,³⁵ the first excited singlet (S_1), adopting just the TDDFT-TDA level of theory. We employed both the PBE0 and B3LYP hybrid functionals. The results obtained with the two functional are slightly different but the overall picture of pathways for FIrpic degradation is the same. In the next section we'll report only the PBE0 results, while B3LYP results are reported the Supplementary Information (SI).

We used the Gaussian03 package³⁶ and the 6-31g(d,p) basis set for the light atoms (hydrogen, carbon, nitrogen, oxygen and fluorine), and the aug-cc-pVDZ basis with 17 valence electrons for Ir. The remaining 60 core electrons were described with by a pseudopotential specifically developed for this basis.³⁷ Our basis set, which includes diffuse as well as polarization functions, should be flexible enough to ensure that the wavefunction might expand on an appropriate set of Gaussian functions even in geometrical conformations far from the closed isomer.

We considered four pathways possibly leading to FIrpic degradation: breaking of Ir-O and Ir-N bonds of the picolate fragment (pic), as well as Ir-N and Ir-C bonds belonging to one of the (4,6-difluorophenyl)pyridinate moieties (F_2 ppy). In a single case we also detailed a complete isomerization pathway through breaking of the bond between iridium and the nitrogen atom belonging to the F_2 ppy fragment. We tried to simulate the isomerization of FIrpic simply by rotating one of the fragments, but we always observed further bond breaking during the calculations.

All configurations presented here have been fully relaxed. The effect of zero-point vibrational motion on the estimate of energy barriers and stability of open conformations has been evaluated in selected geometries, and proved almost negligible (i.e. of the order of 0.01 eV). This correction is therefore not included in the data reported in the next section. Transition states were determined using analytical derivatives in the case of DFT single determinant computations, while TDDFT data came from numerical scans over the reaction coordinates, where all internal coordinates but one were optimized.

Dynamical simulations

We carried out Car-Parrinello³⁰ molecular dynamics simulations of FIrpic imposing constrained occupations to simulate the presence of an electronic excitation. These simulations were performed with the CPV code of Quantum Espresso.^{38,39}

We used ultrasoft pseudopotentials with a plane-wave energy cut-off of 45.6 Ry, and the PBE functional. Isolated molecules are contained in a supercell with at least 10 Å of vacuum around the starting geometrical configuration. Equation of motion of ions and electrons were integrated with the Verlet algorithm, assigning to the electron a fictitious mass of 400 atomic units. To control the dynamics we used a Nosé thermostat with a temperature of 1000 K for ions, acting with a frequency of 90 THz. This same thermostat, acting with a frequency of 110 THz, has been adopted for electrons in the simulations of polarons and excitons, keeping as reservoir the asymptotic value of the electronic kinetic energy obtained in the neutral-ground state computation. For each system we performed 90,000 steps of molecular dynamics, which correspond to an overall time evolution of ~ 11 ps. A temperature as high as 1000 K might seem unrealistic, and its sole purpose is to speed up the dynamical evolution. In any case, we verified that such high temperature does not induce molecular fragmentation in FIrpic, within the timescale of the simulation.

Results and discussion

Static computations: Ring opening and isomerization

We report our energetic analysis concerning ligand opening and isomerization of FIrpic in Tab. 1. A schematic view of the most relevant transition paths for Ir-ligand bond breaking is depicted in Fig. 2, and a selected set of conformations is showed in Fig. 3 and Fig. 4.

Let us begin with the closed conformation of the most stable isomer (named *closed*), which we take as a reference through the entire discussion (see Fig. 1). Electronic excitation

has little effect on the relative geometrical arrangement of the ligands, and the same holds true for internuclear distances of bonds formed by iridium with F₂ppy moieties. As concerns the picolate fragment, excitation of the molecule to a triplet state induces a small but noticeable elongation of the Ir-N bond (about 0.05 Å), while in the first excited singlet the Ir-O bond shortens by ~ 0.1 Å, of by ~ 0.01 Å in the first triplet state. Our results agree very well with previous calculations reported in literature.^{12,40}

Table 1: Relative energies (eV) of several FIrpic conformations with respect to the closed ground state minimum. All conformations are fully relaxed. Data obtained with the PBE0 functional.

Geometry	Ground state	Triplet	Exciton triplet	Exciton singlet
Closed	0.000	2.722	2.682	2.692
N-pic TS ^a	1.150	3.094	3.130	3.514
N-pic open	0.444	2.846	2.882	3.245
O-pic TS	no state	no state	3.800	3.986
O-pic open	no state	no state	3.729	3.752
C-F ₂ ppy TS	5.194	4.886	4.972	5.597
C-F ₂ ppy open	5.144	4.792	4.794	4.873
N-F ₂ ppy TS (open \rightarrow A)	no state	3.102	3.176	3.687
N-F ₂ ppy open (A)	no state	2.988	3.031	3.673
N-F ₂ ppy TS (A \rightarrow B)	2.446 ^b	3.859	3.830	4.231
N-F ₂ ppy open (B)	1.819	3.077	3.086	3.562
N-F ₂ ppy TS (B \rightarrow isomer)	2.586	3.308	3.299	3.602

^a TS is an acronym for transition state. ^b The transition state in this case corresponds to the transition from the closed geometry to the state B.

The bonds between Ir and the ligands have quite different strength, and opening of the picolate fragment is much more viable through breaking of Ir-N as compared to Ir-O. When the molecule is in its ground state (GS), this process requires 1.150 eV (111 kJ/mol), a value reduced to 0.822 eV (79 kJ/mol) when the first excited singlet is considered. When the molecule is in the lowest triplet, a much smaller activation energy is needed: 0.372 eV (36 kJ/mol) as estimated by single determinant (SD) triplet computations, and 0.448 eV (43 kJ/mol) at TDDFT level. The metastable open state is very stable in the GS, 0.706 eV below the transition barrier. Furthermore, once N detaches from Ir, the two oxygen atoms

rearrange and both become ligands of the metal atom, whose coordination remains essentially a distorted octahedron.

The situation is quite different as far as excited electronic states are considered. First, open conformations obtained by Ir-N bond breaking reside about 0.25 eV (24 kJ/mol) below the transition barrier. Second, upon breaking of Ir-N bond the Ir abandons the distorted octahedral conformation of the closed molecule and becomes a trigonal bipyramid, where Ir has just five ligands and the open pyridine fragment moves far away from the bonding region with Ir. When the molecule is electronically excited, the geometrical arrangement of fragments in the transition state (TS) is similar to the corresponding open minimum. The most significant difference comes from the torsion angle between CO₂ and pyridine within the picolate fragment, which is very small either in closed and open conformations and somewhat larger in TS. Its value ranges from 7° considering the transition state of the electronic ground state to about 20° when electron excitations are considered.

Elongation of the Ir-O bond leads to no metastable conformation in the ground state Irpic molecule. As for the spin triplet, an open state might not exist, as predicted by single-determinant computations, or be very shallow, less than 0.1 eV below the barrier at the TDDFT level, a value comparable to the thermal energy at 300 K. The opening barrier is significantly higher in the excited singlet than in the triplet, 1.294 eV (124 kJ/mol) to be compared with 1.118 eV (107 kJ/mol), but the open state is markedly deeper in the first case, 0.234 eV (22 kJ/mol) below the TS. In the open state generated by elongation of Ir-O bonds, a relevant torsion between the CO₂ and the pyridine fragments of picolate occurs, and reaches up to 50°. At the same time, pyridine rotates away from the C-Ir-C plane by about 20°.

Let us now consider the opening of the F₂ppy ligand. The bond with carbon is the strongest among the ones formed by the central Ir atom. When the molecule is in its electronic ground state, ring opening at Ir-C has an exceedingly high barrier, larger than 5 eV. Electron excitation into a singlet state reduces this value to about 3 eV, and the

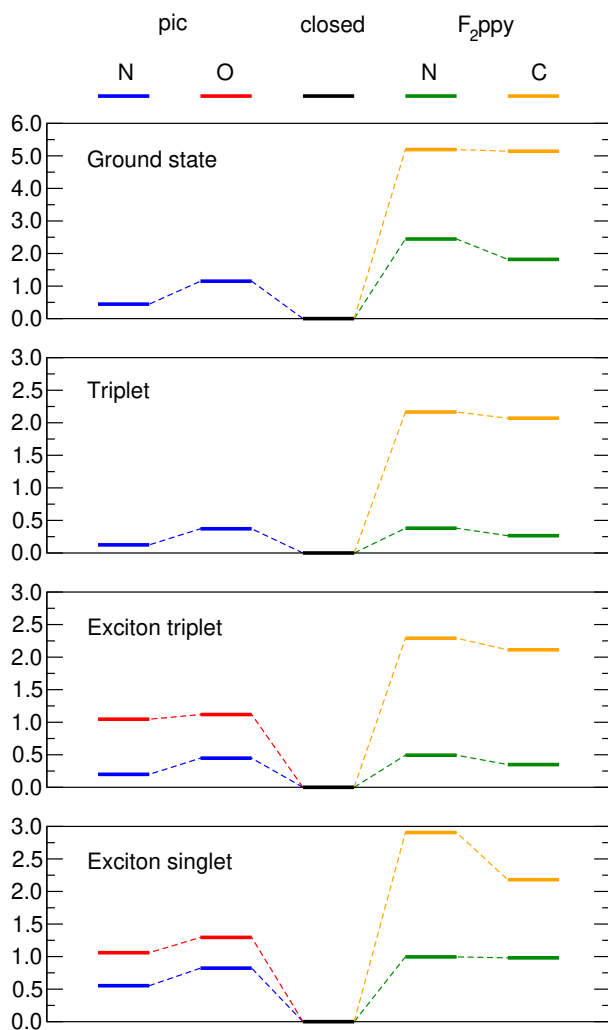


Figure 2: Relative energies (eV) of transition and metastable open states of FIrpic, determined for several electronic states (see caption in each panel). For convenience, the energy of each closed conformation is set to zero. The opening of the picolinate fragment is reported on the left, while the opening of the (4,6-difluorophenyl)pyridinate (F_2ppy) is reported on the right. Every structure is fully relaxed. Data obtained with the PBE0 functional.

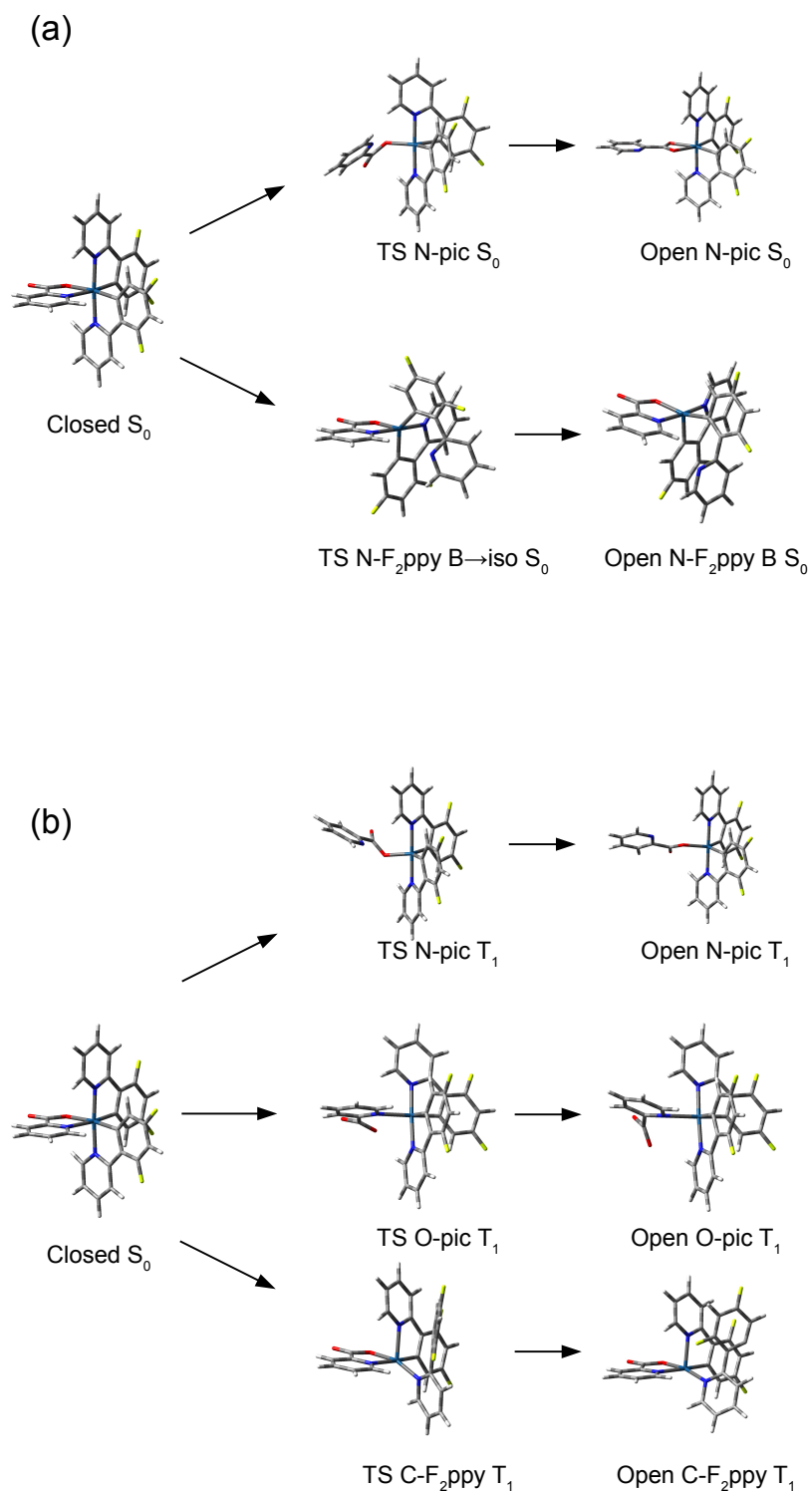


Figure 3: Selected conformations of FIrpic relevant to ligand opening. (a) Ir-N(pic) and Ir-N(F₂ppy) opening in the ground state (S_0). (b) Ir-N(pic), Ir-O(pic) and Ir-C(F₂ppy) opening in the excited triplet (T_1). All structures are fully relaxed. Data obtained with the PBE0 functional.

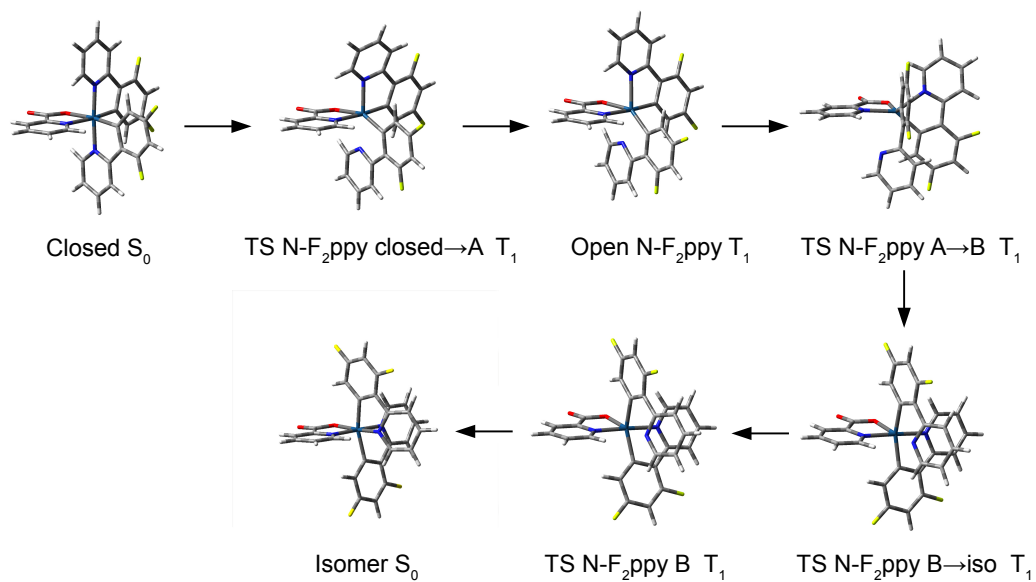


Figure 4: Selected conformations of FIrpic relevant to isomerization, in the T_1 state. All structures are fully relaxed. Data obtained with the PBE0 functional.

activation energy further reduces to slightly more than 2 eV in the first triplet excited state. The open metastable state is quite shallow as far as the GS and the triplet excitation are considered, while it is very deep (0.724 eV, 70 kJ/mol) in the first excited singlet. As for the conformation, after Ir-C breaking FI_{irpic} evolves towards a square base pyramid. The open F₂phenyl fragment presents a torsion angle with pyridine of 56° in the GS. This value is largely increased in the excited states: 122° in the excited singlet, 124° in the exciton singlet and 138° in the SD triplet. Transition states between open and closed Ir-C conformations are characterized by a moderate distortion of the square pyramid (the N-Ir-N bond angle involving F₂ppy fragments slightly increases from about 110° to 120°), while a strong reduction of the torsion between open F₂phenyl group and pyridine occurs.

Opening of Ir-N bonds of F₂ppy requires to overcome energy barriers comparable to the analogous bond of picolinate. Moreover, when the molecule is electronically excited, this process represents a feasible way towards isomerization of FI_{irpic}, involving two different intermediate states. Indeed, the elongation of Ir-N leads to a first metastable conformation (labelled A in Table 1) which is not present in the GS molecule. In state A, both Ir-N bonds of F₂phenyl increase their internuclear distance, about 0.4 and 0.2 Å for the opening and the closed ligands, respectively. The related N-Ir-N bond angle markedly decreases from about 180° to about 145° (excited triplet) and 163° (excited singlet). The excited triplet has a barrier smaller than 0.5 eV (48 kJ/mol), and a large stability of the open states (about 0.5 eV below the barrier). Conversely, the excited singlet has a large barrier, about 1 eV, and a negligible stability range. Considering that no analogous metastable state is found for the molecule in the singlet ground state, we argue that intermediate state A is stabilized by a spin triplet electronic configuration. Once the Ir-N bond elongates up to about 2.5 Å to reach conformation A, the system can evolve towards a second metastable state, which has been found also when the molecule is in its electronic ground state, and is labelled as B in Table 1 and Fig. 4. Interestingly, in state B the relative conformation of picolinate and closed F₂ppy fragment does not correspond anymore to the starting closed FI_{irpic} isomer, but

closely mimics the arrangement of a different isomer. The rearrangement of the picolate and the closed F₂ppy fragments occurring in state B induces steric hindrance on the open F₂ppy fragment, which counteracts either by rotating the open pyridine with respect to the difluoro-phenyl group, as occurs in the ground state, or by rotating the entire F₂ppy fragment towards a spatial region free of atoms, as happens in the excited states.

Considering the GS molecule, the activation energy required to evolve from the closed to the B metastable state is very high, 2.446 eV (236 kJ/mol). However, when the system is electronically excited, energy barriers from A to B are much smaller, less than 0.8 eV. Moreover, the B conformation is very stable with respect to the A to B transition state, about 0.5 eV below the top of the barrier. Transition states between A and B are characterized by a relative arrangement between the picolate and the closed F₂ppy fragments half the way between the initial and final closed isomers. Indeed, the relative N-Ir-N angle measures about 140°, to be compared with 90° in the minimum energy starting isomer, and 180° in the final closed isomer. Once the open state labeled as B is formed, the evolution towards the final closed isomer requires smaller barriers than the previous steps: 0.767 eV (74 kJ/mol) in the GS, a value that decreases to about 0.2 eV (19 kJ/mol) in the excited triplet and to 0.04 eV (4 kJ/mol) in the excited singlet. Overall, isomerization along the described path requires at least 2.5 eV (241 kJ/mol) when FIrpic is in the GS, but when the molecule is in its first excited singlet the activation energy required is 1 eV smaller, a value further reduced to about 1.1 eV (106 kJ/mol) when the molecule is excited to a triplet state. Finally, we note that people have argued and shown, that different isomers might display different non-radiative channels due to their complex excited state PES.^{24,41,42}

Car-Parrinello simulations

First, we performed ab-initio molecular dynamics (MD) runs of FIrpic in the neutral, positively and negatively charged state. These runs revealed that no rearrangements but thermal motion takes place, and that the ligands around Ir retain the conformation of a distorted

octahedra. This is consistent with static computations, since in the neutral GS molecule bond breaking involving Ir and its ligands requires activation energies larger than 1 eV, a value much higher than vibrational energy at 1000 K.

The above picture radically changes when the non-spin-polarized exciton is considered. Indeed, in two out of three MD runs of this systems, we observed breaking of bonds between the metal atom and one ligand, and even complete fragmentation of the molecule. In this section we'll describe extensively just one of the three simulations (from now on referred to as Simulation I), while the other two (Simulations II and III) are only briefly reviewed. We report our results on Simulation I in Fig. 5, while the raw data from the entire set of simulations are reported in the SI. In Fig. 6 we report four snapshots of the MD trajectory extracted from the *c*-CPMD simulation of the exciton.

As can be seen in Fig. 5, the relevant structural parameters (i.e. Ir-X bond lengths and X-Ir-X bond angles) remain quite constant up to 4.05 ps, when the Ir-N bond involving the picolinate fragment suddenly starts elongating. Once Ir-N is longer than ~ 4 Å, an important change in the overall conformation of FIrpic takes place. Indeed, as can be seen in the bottom panel of Fig. 5, the C-Ir-O bonding angles (where carbon atoms belong to the F₂ppy fragments, and oxygen to picolinate) become similar to each another. This is consistent with static computations where, upon Ir-N bond breaking at the picolinate fragment, FIrpic abandons the octahedral conformation and becomes a distorted trigonal bipyramid, characterized by almost equal C-Ir-O angles.

At 5.20 ps the elongation of Ir-N and the rearrangement of the ligands around the central metal atom induces a second and quite unexpected effect on the conformation of FIrpic. Indeed, the oxygen atom not bonded to Ir approaches the metal, and at 5.85 ps Ir-O shortens up to about 2 Å, the typical bonding distance between iridium and oxygen. At the same time lapse, the oxygen atom formerly bonded to Ir moves away from the central metal atom reaching an internuclear distance of about 3.5 Å, where the bond with the metal is practically broken. According to static computations, this process requires a very small

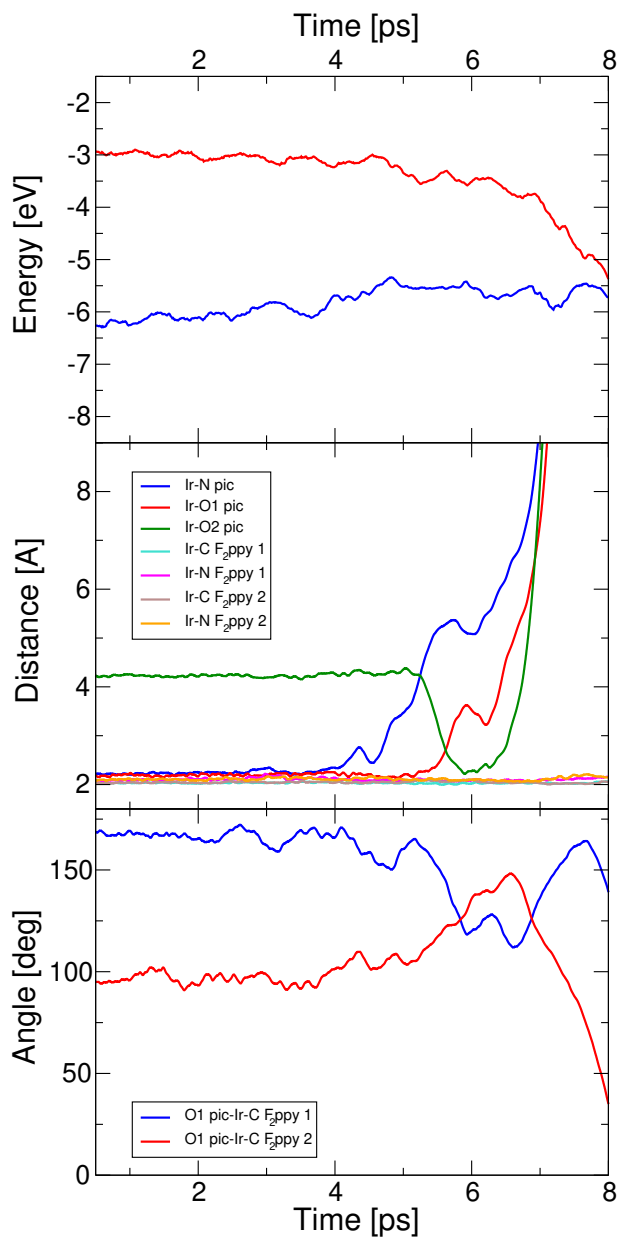


Figure 5: Dynamical evolution of energetic and structural parameters of FIrpic as extracted from CP Simulation I. Top panel: eigenvalues (eV) of the highest singly occupied molecular orbitals. Middle panel: internuclear distances (\AA) between iridium and the six ligands, plus the separation between Ir and the second oxygen of the picolinate fragment (O2). Bottom panel: angles (degrees) formed by the oxygen atom bonded to iridium (O1), the central metal atom, and the carbon atoms belonging to the F_2ppy fragment and bonded to Ir. We made the plots smoother and more readable by averaging values over 25 data points.

activation energy: 0.16 eV considering the single-determinant triplet, 0.11 and 0.14 eV at TDA level for the first singlet and triplet excited states, respectively.

Then the molecule reaches a kind of steady state at about 5.95 ps, when Ir-N measures about 5.5 Å, and the nitrogen too distant from Ir in order to form a chemical bond. At this time step the two oxygen atoms of the picolinate fragment swap their positions as ligands of the central metal atom, which forms just five bonds instead of the six present in the starting closed conformation. Angles between carbon, iridium and oxygen confirm that the molecule is closer to a trigonal bipyramid rather than to an octahedron. Few picoseconds later, more precisely at 6.25 ps, elongation of Ir-N takes place again and the same happens for both Ir-O distances. The picolinate fragment abandons FIrpic.

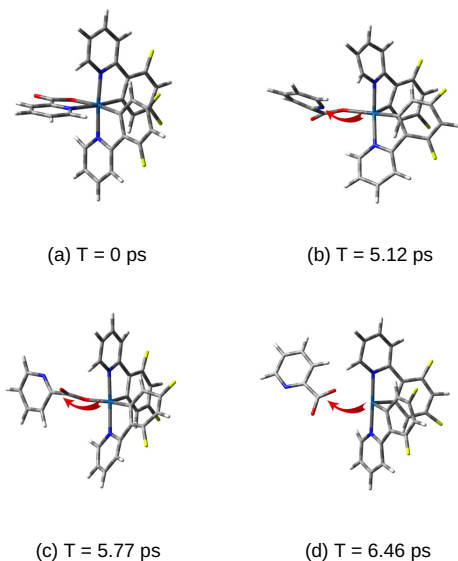


Figure 6: Selected snapshots of the CP dynamics of FIrpic in the first excited state. (a) Starting closed conformation; (b) The Ir-N bond elongates and nitrogen detaches from iridium; (c) The oxygen atom bonded to iridium detaches and is substituted by the second carboxylate oxygen; (d) The Ir-O bond elongates and the entire picolinate fragment abandons FIrpic, thus leading to irreversible degradation.

We also note that the frontier (HOMO/LUMO) eigenvalues of FIrpic remain quite sep-

arated from one another during the MD run, until the picolinate fragment is lost. This suggests that fast, non-radiative recombination is not likely to occur. Moreover, the driving mechanism of fragmentation originates from breaking of Ir-N involving the picolinate fragment, which according to static computations is the weakest bond among the six formed by the metal atom.

Simulation II shows essentially the same mechanisms discussed above. Ir-N opening at the picolinate fragment starts at 2.5 ps, and about 0.5 ps later the two oxygen atoms swap as ligand of iridium. The short Ir-O bond elongates up to about 4 Å, and the oxygen not bonded to iridium substitutes the former one as metal ligand. Quite interestingly, in Simulation II the two oxygens swap again their relative position with respect to Ir before the fragmentation of FIrpic takes place. This phenomenon manifests at 4.7, 5.2 and 6.0 ps, and no dissociation of the picolinate fragment from iridium takes place until 7.8 ps. Its driving force is also in this case a sudden elongation of Ir-N. Differently from simulation I, in this case the frontier eigenvalues gets very close to each other even before fragmentation, which implies that fast non-radiative recombination should not be ruled out.

In simulation III we observed a quite different behavior with respect to the other two. First of all, elongation and breaking of Ir-N is not followed by the exchange between the two oxygens as Ir ligands. Indeed, they swap position shortly twice, at 9.0 and 9.7 ps, quite a long time after breaking of Ir-N, which occurs at 3.1 ps. Second, no fragmentation is observed, and FIrpic is left, for quite a long time (7.7 ps), with just five ligands around Ir instead of six. Here, fragmentation does not appear to be a necessary consequence of ring opening. Third, as observed in simulation II the frontier eigenvalues approach each other after breaking of Ir-N.

A final comment concerning all MD three runs on FIrpic is mandatory. Once Ir-N is broken, the unbound pyridine group of picolinate should be free to rotate, as no relevant steric hindrance should be encountered. As a matter of fact, the torsion of this group with respect to the carboxyl group is somewhat correlated to the relative position of the oxygen

atoms with respect to Ir, such as the nitrogen atom gets as close as possible to the oxygen bound to iridium.

After the dissociation of the picolinate we also observed detachment of a CO₂ molecule from the picolinate (reported in literature), leaving a C₅H₄N⁺ fragment. However the closing of the HOMO-LUMO gap, the Car-Parrinello method is not suitable to describe non-adiabatic effects, hence our observation of the CO₂ molecule evolution in a very short timescale (few ps) could be an artifact of the method.

Before closing, we would like to highlight two points: the first is that the rather high temperature in simulations (1000 K \simeq 0.083 eV) was used only to accelerate the dynamics. We verified that in the neutral state at 1000 K, FIrpic remains intact for the duration of the simulation. Thus, the simulation temperature has a little influence on the electronic excitations, and thermal dissociation might occur on longer time-scales.

The second is that our CPMD simulations are not meant to reproduce a statistical ensemble in thermal equilibrium. Rather, they represent a tool to generate and explore possible degradation paths. Indeed we cannot extract lifetimes from our simulations, as non-adiabatic effects are not described accurately by the method. The lack of statistical sampling means that the method cannot predict the relative probability of each single degradation event.

Conclusions

In this paper we unraveled the degradation mechanism of FIrpic by means of theoretical computations, and we also identified a possible pathway for its isomerization. Ab-initio molecular dynamics simulations predict the no degradation occurs when the molecule is in the ground state, and the same holds true when FIrpic is positively or negatively charged. Static computations confirm this outcome, since bond breaking between the central metal atom and its ligands requires activation energies ranging from 1 to 5 eV depending on the

bond considered.

The picture radically changes when an excited electronic configuration is considered. All bonds formed by Ir become weaker, and the Ir-N ones become the loosest. Static computations indicate that when the molecule is excited in its triplet state, breaking of the Ir-N at the picolate and the F₂ppy fragments requires an activation energy of about 0.5 eV, while about 1 eV is needed when in the first excited singlet. Interestingly, in our Car-Parrinello simulations of the excited molecule we invariably observed Ir-N breaking at the picolate fragment, followed by formation of a metastable open intermediate with a distorted trigonal bipyramidal arrangement of the ligands around iridium. Molecular dynamics simulations also showed that after Ir-N opening, the two oxygens of picolate reversibly swap as ligands of iridium, which thereafter remains five-fold coordinated.

This process paved the way towards fragmentation of FIrpic, which loses the picolate fragment in two simulations out of three, a result in nice agreement with the general consensus on this subject. As a further confirmation of this picture, in a parallel experimental investigation (Paper II⁴³) we proved that the loss of picolate is indeed the key step in the degradation of FIrpic based devices. Furthermore, we discovered that the resulting Ir(F₂ppy)⁺ species favorably bind to BPhen, a material widely used as electron transport layer in OLED devices. Remarkably, the electron emission spectrum of [Ir(F₂ppy)₂BPhen]⁺ is significantly redshifted with respect to the unaged FIrpic. This outcome has been confirmed by static computations conducted on this molecule at the same level of theory adopted for FIrpic.

Another fallout of the aging of FIrpic based devices is isomerization. Contrary to previous computational investigations, we proved that isomerization cannot be afforded simply by rotating the moieties bonded to iridium. Indeed, the first step is necessarily the opening of one Ir-ligand bond, followed by a quite complex conformational rearrangement of the entire molecule. The overall energy barrier for the isomerization of the ground state FIrpic molecule is about 2.5 eV, a value reduced to about 1 eV when the first excited singlet and

triplet states are considered.

In conclusion, by means of state of the art computations we provided a rationale for the degradation and isomerization mechanisms of FIrpic, which go through the same initial steps. Consistently with experimental evidences, it comes out that at real operating temperatures both processes are viable only when the molecule is electronically excited, and more so when the first excited triplet is considered. Overall, our results provide a solid physical basis to establish the relation between the excitation/de-excitation processes and the degradation of FIrpic in OLED devices.

Acknowledgement

We acknowledge the CINECA award under the ISCRA initiative, for the availability of high performance computing resources and support (Grants Nr. HP10CH6GBY, HP10CKPLJY and HP10CJYU54). This project was funded by the GRO 2014 and 2015 program of Samsung Advanced Institute of Technology (SAIT). We thank Woon-jon Son, Dongseon Lee and Rocco Martinazzo for useful discussions.

Supporting Information Available

The following files are available free of charge. Additional results from static computations performed at the B3LYP level and c-CPMD simulations results for three different trajectories simulating the exciton.

References

- (1) Minaev, B.; Baryshnikov, G.; Agren, H. Principles of phosphorescent organic light emitting devices. *Phys. Chem. Chem. Phys.* **2014**, *16*, 1719–1758, DOI: 10.1039/C3CP53806K.

- (2) Scholz, S.; Kondakov, D.; Lssem, B.; Leo, K. Degradation Mechanisms and Reactions in Organic Light-Emitting Devices. *Chemical Reviews* **2015**, *115*, 8449–8503, DOI: 10.1021/cr400704v.
- (3) Kang, J.-W.; Lee, S.-H.; Park, H.-D.; Jeong, W.-I.; Yoo, K.-M.; Park, Y.-S.; Kim, J.-J. Low roll-off of efficiency at high current density in phosphorescent organic light emitting diodes. *Applied Physics Letters* **2007**, *90*, 223508, DOI: 10.1063/1.2745224.
- (4) Sajoto, T.; Djurovich, P. I.; Tamayo, A. B.; Oxgaard, J.; Goddard, W. A.; Thompson, M. E. Temperature Dependence of Blue Phosphorescent Cyclometalated Ir(III) Complexes. *Journal of the American Chemical Society* **2009**, *131*, 9813–9822, DOI: 10.1021/ja903317w.
- (5) Forrest, S. R. Excitons and the lifetime of organic semiconductor devices. *Philosophical Transactions of the Royal Society of London A: Mathematical, Physical and Engineering Sciences* **2015**, *373*, DOI: 10.1098/rsta.2014.0320.
- (6) Schmidbauer, S.; Hohenleutner, A.; Knig, B. Chemical Degradation in Organic Light-Emitting Devices: Mechanisms and Implications for the Design of New Materials. *Advanced Materials* **2013**, *25*, 2114–2129, DOI: 10.1002/adma.201205022.
- (7) de Moraes, I. R.; Scholz, S.; Lssem, B.; Leo, K. Analysis of chemical degradation mechanism within sky blue phosphorescent organic light emitting diodes by laser-desorption/ionization time-of-flight mass spectrometry. *Organic Electronics* **2011**, *12*, 341 – 347, DOI: 10.1016/j.orgel.2010.11.004.
- (8) Citti, C.; Battisti, U. M.; Ciccarella, G.; Maiorano, V.; Gigli, G.; Abbate, S.; Mazzeo, G.; Castiglioni, E.; Longhi, G.; Cannazza, G. Analytical and preparative enantioseparation and main chiroptical properties of Iridium(III) bis(4,6-difluorophenylpyridinato)picolinato. *Journal of Chromatography A* **2016**, *1467*, 335 – 346, DOI: 10.1016/j.chroma.2016.05.059.

- (9) Baranoff, E.; Curchod, B. F. E. FIrpic: archetypal blue phosphorescent emitter for electroluminescence. *Dalton Trans.* **2015**, *44*, 8318–8329, DOI: 10.1039/C4DT02991G.
- (10) Himmetoglu, B.; Marchenko, A.; Dabo, I.; Cococcioni, M. Role of electronic localization in the phosphorescence of iridium sensitizing dyes. *The Journal of Chemical Physics* **2012**, *137*, 154309, DOI: 10.1063/1.4757286.
- (11) Wang, L.; Wu, Y.; Shan, G.-G.; Geng, Y.; Zhang, J.-Z.; Wang, D.-M.; Yang, G.-C.; Su, Z.-M. The influence of the diphenylphosphoryl moiety on the phosphorescent properties of heteroleptic iridium(III) complexes and the OLED performance: a theoretical study. *J. Mater. Chem. C* **2014**, *2*, 2859–2868, DOI: 10.1039/C3TC31831A.
- (12) Li, H.; Winget, P.; Risko, C.; Sears, J. S.; Bredas, J.-L. Tuning the electronic and photophysical properties of heteroleptic iridium(III) phosphorescent emitters through ancillary ligand substitution: a theoretical perspective. *Phys. Chem. Chem. Phys.* **2013**, *15*, 6293–6302, DOI: 10.1039/C3CP50631B.
- (13) Escudero, D.; Jacquemin, D. Computational insights into the photodeactivation dynamics of phosphors for OLEDs: a perspective. *Dalton Transactions* **2015**, *44*, 8346–8355, DOI: 10.1039/C4DT03804E.
- (14) Li, J.; Zhang, Q.; He, H.; Wang, L.; Zhang, J. Tuning the electronic and phosphorescence properties of blue-emitting iridium(III) complexes through different cyclometalated ligand substituents: a theoretical investigation. *Dalton Trans.* **2015**, *44*, 8577–8589, DOI: 10.1039/C5DT00048C.
- (15) Xu, S.; Wang, J.; Xia, H.; Zhao, F.; Wang, Y. Computational prediction for emission energy of iridium (III) complexes based on TDDFT calculations using exchange correlation functionals containing various HF exchange percentages. *Journal of Molecular Modeling* **2015**, *21*, 22, DOI: 10.1007/s00894-014-2557-1.

- (16) Kesarkar, S.; Mrz, W.; Penconi, M.; Pasini, M.; Destri, S.; Cazzaniga, M.; Ceresoli, D.; Mussini, P. R.; Baldoli, C.; Giovanella, U.; Bossi, A. Near-IR Emitting Iridium(III) Complexes with Heteroaromatic -Diketonate Ancillary Ligands for Efficient Solution-Processed OLEDs: StructureProperty Correlations. *Angewandte Chemie International Edition* **55**, 2714–2718, DOI: 10.1002/anie.201509798.
- (17) Jacquemin, D.; Escudero, D. The short device lifetimes of blue PhOLEDs: insights into the photostability of blue Ir(iii) complexes. *Chem. Sci.* **2017**, *8*, 7844–7850, DOI: 10.1039/c7sc03905k.
- (18) Penconi, M.; Cazzaniga, M.; Kesarkar, S.; Mussini, P. R.; Ceresoli, D.; Bossi, A. Upper limit to the ultimate achievable emission wavelength in near-IR emitting cyclometalated iridium complexes. *Photochem. Photobiol. Sci.* **2017**, *16*, 1220–1229, DOI: 10.1039/C7PP00119C.
- (19) Penconi, M.; Cazzaniga, M.; Kesarkar, S.; Baldoli, C.; Mussini, P. R.; Ceresoli, D.; Bossi, A. -Diketonate ancillary ligands in heteroleptic iridium complexes: a balance between synthetic advantages and photophysical troubles. *Photochem. Photobiol. Sci.* **2018**, *17*, 1169–1178, DOI: 10.1039/C8PP00052B.
- (20) Zhang, X.; Jacquemin, D.; Peng, Q.; Shuai, Z.; Escudero, D. General Approach To Compute Phosphorescent OLED Efficiency. *The Journal of Physical Chemistry C* **2018**, *122*, 6340–6347, DOI: 10.1021/acs.jpcc.8b00831.
- (21) Jeong, C.; Coburn, C.; Idris, M.; Li, Y.; Djurovich, P. I.; Thompson, M. E.; Forrest, S. R. Understanding molecular fragmentation in blue phosphorescent organic light-emitting devices. *Organic Electronics* **2019**, *64*, 15–21, DOI: 10.1016/j.orgel.2018.10.001.
- (22) Gabin, T.; Junji, M.; Masayoshi, Y.; Shinichiro, N. Blue Phosphorescent Iridium(III)

- Complex. A Reaction Path on the Triplet Potential Energy Surface. *Chemistry Letters* **2007**, *36*, 1344–1345, DOI: 10.1246/c1.2007.1344.
- (23) Koseki, S.; Kamata, N.-o.; Asada, T.; Yagi, S.; Nakazumi, H.; Matsushita, T. SpinOrbit Coupling Analyses of the Geometrical Effects on Phosphorescence in Ir(ppy)₃ and Its Derivatives. *The Journal of Physical Chemistry C* **2013**, *117*, 5314–5327, DOI: 10.1021/jp312032s.
- (24) Arroliga-Rocha, S.; Escudero, D. Facial and Meridional Isomers of Tris(bidentate) Ir(III) Complexes: Unravelling Their Different Excited State Reactivity. *Inorganic Chemistry* **2018**, *57*, 12106–12112, DOI: 10.1021/acs.inorgchem.8b01675.
- (25) Hedin, L. New Method for Calculating the One-Particle Green’s Function with Application to the Electron-Gas Problem. *Phys. Rev.* **1965**, *139*, A796–A823, DOI: 10.1103/PhysRev.139.A796.
- (26) Aryasetiawan, F.; Gunnarsson, O. The GW method. *Reports on Progress in Physics* **1998**, *61*, 237, DOI: 10.1088/0034-4885/61/3/002.
- (27) Li, X.; Tully, J. C.; Schlegel, H. B.; Frisch, M. J. Ab initio Ehrenfest dynamics. *The Journal of Chemical Physics* **2005**, *123*, 084106, DOI: 10.1063/1.2008258.
- (28) Tully, J. C.; Preston, R. K. Trajectory Surface Hopping Approach to Nonadiabatic Molecular Collisions: The Reaction of H⁺ with D₂. *The Journal of Chemical Physics* **1971**, *55*, 562–572, DOI: 10.1063/1.1675788.
- (29) Barbatti, M.; Granucci, G.; Persico, M.; Ruckebauer, M.; Vazdar, M.; Eckert-Maksi, M.; Lischka, H. The on-the-fly surface-hopping program system Newton-X: Application to ab initio simulation of the nonadiabatic photodynamics of benchmark systems. *Journal of Photochemistry and Photobiology A: Chemistry* **2007**, *190*, 228 – 240, DOI: 10.1016/j.jphotochem.2006.12.008, Theoretical Aspects of Photoinduced Processes in Complex Systems.

- (30) Car, R.; Parrinello, M. Unified Approach for Molecular Dynamics and Density-Functional Theory. *Phys. Rev. Lett.* **1985**, *55*, 2471–2474, DOI: 10.1103/PhysRevLett.55.2471.
- (31) Serra, S.; Tosatti, E.; Iarlari, S.; Scandolo, S.; Santoro, G. Interchain electron states in polyethylene. *Phys. Rev. B* **2000**, *62*, 4389–4393, DOI: 10.1103/PhysRevB.62.4389.
- (32) Serra, S.; Iarlari, S.; Tosatti, E.; Scandolo, S.; Righi, M.; Santoro, G. Self-trapping vs. non-trapping of electrons and holes in organic insulators: polyethylene. *Chemical Physics Letters* **2002**, *360*, 487 – 493, DOI: 10.1016/S0009-2614(02)00832-1.
- (33) Ceresoli, D.; Tosatti, E.; Scandolo, S.; Santoro, G.; Serra, S. Trapping of excitons at chemical defects in polyethylene. *The Journal of Chemical Physics* **2004**, *121*, 6478–6484, DOI: 10.1063/1.1783876.
- (34) Ceresoli, D.; Righi, M. C.; Tosatti, E.; Scandolo, S.; Santoro, G.; Serra, S. Exciton self-trapping in bulk polyethylene. *Journal of Physics: Condensed Matter* **2005**, *17*, 4621, DOI: 10.1088/0953-8984/17/29/004.
- (35) Hirata, S.; Head-Gordon, M. Time-dependent density functional theory within the TammDancoff approximation. *Chemical Physics Letters* **1999**, *314*, 291 – 299, DOI: [https://doi.org/10.1016/S0009-2614\(99\)01149-5](https://doi.org/10.1016/S0009-2614(99)01149-5).
- (36) Frisch, M. J. et al. Gaussian 03. Gaussian, Inc.: Wallingford, CT, 2004.
- (37) Figen, D.; Peterson, K. A.; Dolg, M.; Stoll, H. Energy-consistent pseudopotentials and correlation consistent basis sets for the 5d elements HfPt. *The Journal of Chemical Physics* **2009**, *130*, 164108, DOI: 10.1063/1.3119665.
- (38) Giannozzi, P. et al. QUANTUM ESPRESSO: a modular and open-source software project for quantum simulations of materials. *Journal of Physics: Condensed Matter* **2009**, *21*, 395502.

- (39) Giannozzi, P. et al. Advanced capabilities for materials modelling with Q uantum ESPRESSO. *Journal of Physics: Condensed Matter* **2017**, *29*, 465901, DOI: 10.1088/1361-648X/aa8f79.
- (40) Gu, X.; Fei, T.; Zhang, H.; Xu, H.; Yang, B.; Ma, Y.; Liu, X. Theoretical Studies of Blue-Emitting Iridium Complexes with Different Ancillary Ligands. *The Journal of Physical Chemistry A* **2008**, *112*, 8387–8393, DOI: 10.1021/jp8026429.
- (41) Setzer, T.; Lennartz, C.; Dreuw, A. A theoretical study on the mechanistic highlights behind the Brønsted-acid dependent mer–fac isomerization of homoleptic carbene iridium complexes for PhOLEDs. *Dalton Transactions* **2017**, *46*, 7194–7209, DOI: 10.1039/c7dt01201b.
- (42) Yao, C.; Yang, Y.; Li, L.; Bo, M.; Peng, C.; Wang, J. Not All Bis[2-(4,6-difluorophenyl)pyridyl-N,C2]iridium(III) Picolate (FIrpic) Isomers Are Unsuitable for Developing Long-Lifetime Blue Phosphorescent Organic Light-Emitting Diodes. *The Journal of Physical Chemistry C* **2019**, *123*, 227–232, DOI: 10.1021/acs.jpcc.8b10599.
- (43) Penconi, M.; Cazzaniga, M.; Panzeri, W.; Mele, A.; Cargnoni, F.; Ceresoli, D.; Bossi, A. Unraveling the degradation mechanism in FIrpic based blue OLEDs: II. Trap and detect molecules at the interfaces. *Chemistry of Materials* **2019**,

Graphical TOC Entry

